# VARIABLE HORIZON IN A PERIDYNAMIC MEDIUM

S. A. SILLING, D. J. LITTLEWOOD, AND P. SELESON

Abstract. A notion of material homogeneity is proposed for peridynamic bodies with variable horizon but constant bulk properties. A relation is derived that scales the force state according to the position-dependent horizon while keeping the bulk properties unchanged. Using this scaling relation, if the horizon depends on position, artifacts called ghost forces may arise in a body under a homogeneous deformation. These artifacts depend on the second derivative of the horizon and can be reduced by employing a modified equilibrium equation using a new quantity called the *partial stress*. Bodies with piecewise constant horizon can be modeled without ghost forces by using a simpler technique called a *splice*. As a limiting case of zero horizon, both the partial stress and splice techniques can be used to achieve local-nonlocal coupling. Computational examples, including dynamic fracture in a one-dimensional model with local-nonlocal coupling, illustrate the methods.

## 1. Introduction

The peridynamic theory is a strongly nonlocal formulation of solid mechanics, based on long-range forces, that is adapted to the study of continuous bodies with evolving discontinuities, including cracks [22, 25, 26]. Each material point $\mathbf{x}$ in the reference configuration of a body $\mathcal{B}$ interacts through the material model with other material points within a distance $\delta(\mathbf{x})$ of itself. The maximum interaction distance $\delta(\mathbf{x})$ is called the *horizon* of $\mathbf{x}$. The material points within the horizon of $\mathbf{x}$ comprise a set called the *material family* of $\mathbf{x}$:

$$\mathcal{F}_{\mathbf{x}} = \Big\{ \mathbf{q} \in \mathcal{B} \ : \ 0 < |\mathbf{q} - \mathbf{x}| \leq \delta(\mathbf{x}) \Big\}.$$

The vector from $\mathbf{x}$ to any neighboring material point $\mathbf{q} \in \mathcal{F}_{\mathbf{x}}$ is called a *bond*, $\boldsymbol{\xi} = \mathbf{q} - \mathbf{x}$. The set of bonds from $\mathbf{x}$ to its neighbors within its horizon is called the *family* of $\mathbf{x}$, denoted $\mathcal{H}_{\mathbf{x}}$:

$$\mathcal{H}_{\mathbf{x}} = \Big\{ \boldsymbol{\xi} \in \mathbb{R}^3 \ : \ \mathbf{x} + \boldsymbol{\xi} \in \mathcal{F}_{\mathbf{x}} \Big\}.$$

In an elastic peridynamic solid, the strain energy density $W(\mathbf{x})$ is determined by the collective deformation of $\mathcal{F}_{\mathbf{x}}$. To express this collective deformation, it is convenient to define the function $\underline{\mathbf{Y}}[\mathbf{x}, t]\langle \cdot \rangle : \mathcal{H}_{\mathbf{x}} \to \mathbb{R}^3$ that maps bonds into their images under the deformation $\mathbf{y}$. For any material point $\mathbf{q} \in \mathcal{F}_{\mathbf{x}}$ at time $t$, let

$$\underline{\mathbf{Y}}[\mathbf{x}, t]\langle \mathbf{q} - \mathbf{x} \rangle = \mathbf{y}(\mathbf{q}, t) - \mathbf{y}(\mathbf{x}, t). \tag{1-1}$$

The function $\underline{\mathbf{Y}}[\mathbf{x}, t]\langle \cdot \rangle$ is an example of a *state*, which is a mapping with domain $\mathcal{H}_{\mathbf{x}}$. By convention, the bond in $\mathcal{H}_{\mathbf{x}}$ that a state operates on is written in angle brackets, $\langle \boldsymbol{\xi} \rangle$. $\underline{\mathbf{Y}}[\mathbf{x}, t]$ is called the *deformation state* at $\mathbf{x}$ and at time $t$. The deformation state is the basic kinematical

*Key words and phrases.* Elasticity; Nonlocality; Local-nonlocal coupling; Peridynamics.

Sandia is a multiprogram laboratory operated by Sandia Corporation, a Lockheed Martin Company, for the United States Department of Energy's National Nuclear Security Administration under contract DE-AC04-94AL85000.

quantity for purposes of material modeling and in this role is analogous to the deformation gradient $\mathbf{F} = \partial \mathbf{y}/\partial \mathbf{x}$ in the standard theory.

For convenience in the present discussion, we will adopt the generalization that a state operating on a bond vector outside of the family is defined, but its value is zero:

$$|\boldsymbol{\xi}| > \delta(\mathbf{x}) \quad \Longrightarrow \quad \underline{A}[\mathbf{x}]\langle \boldsymbol{\xi} \rangle = \mathbf{0}.$$

The inner product of two states $\underline{\mathbf{A}}$ and $\underline{\mathbf{B}}$ is defined by

$$\underline{\mathbf{A}} \bullet \underline{\mathbf{B}} = \int_{\mathcal{H}} \underline{\mathbf{A}}\langle \boldsymbol{\xi} \rangle \cdot \underline{\mathbf{B}}\langle \boldsymbol{\xi} \rangle \, dV_{\boldsymbol{\xi}}. \tag{1-2}$$

(In this equation and the rest of this paper, we use the symbol $\mathcal{H}$ instead of $\mathcal{H}_{\mathbf{x}}$ when it is not necessary to refer to a specific $\mathbf{x} \in \mathcal{B}$.) The *norm* of a state $\underline{\mathbf{A}}$ is defined by

$$\|\underline{\mathbf{A}}\| = \sqrt{\underline{\mathbf{A}} \bullet \underline{\mathbf{A}}}.$$

In an elastic material, the strain energy density $W(\mathbf{x})$ depends through the material model on the deformation state, and this dependence is written

$$W(\mathbf{x}) = \hat{W}(\underline{\mathbf{Y}}[\mathbf{x}]).$$

In manipulating functions of states such as $W$, it is helpful to introduce the *Fréchet derivative*. The Fréchet derivative $\hat{W}_{\underline{\mathbf{Y}}}$ is a functional derivative with the property that if $\delta\underline{\mathbf{Y}}$ is a small increment in the deformation state,

$$\hat{W}(\underline{\mathbf{Y}} + \delta\underline{\mathbf{Y}}) = \hat{W}(\underline{\mathbf{Y}}) + \hat{W}_{\underline{\mathbf{Y}}}(\underline{\mathbf{Y}}) \bullet \delta\underline{\mathbf{Y}} + o(\|\delta\underline{\mathbf{Y}}\|). \tag{1-3}$$

(Note that $\hat{W}_{\underline{\mathbf{Y}}}$ is a state-valued function even though $\hat{W}$ is scalar-valued.)

Let $\Phi_{\mathbf{y}}$ denote the total potential energy in a bounded elastic body under external body force density field $\mathbf{b}$, subjected to the deformation $\mathbf{y}$:

$$\Phi_{\mathbf{y}} = \int_{\mathcal{B}} (W(\mathbf{x}) - \mathbf{b}(\mathbf{x}) \cdot \mathbf{y}(\mathbf{x})) \, dV_{\mathbf{x}}. \tag{1-4}$$

To derive the Euler-Lagrange equation corresponding to stationary values of this functional, set the first variation to zero. Combining (1-1), (1-3), and (1-4) leads to

$$\begin{aligned} 0 &= \delta\Phi_{\mathbf{y}} = \int_{\mathcal{B}} (\delta W(\mathbf{x}) - \mathbf{b}(\mathbf{x}) \cdot \delta\mathbf{y}(\mathbf{x})) \, dV_{\mathbf{x}} \\ &= \int_{\mathcal{B}} (\hat{W}_{\underline{\mathbf{Y}}}[\mathbf{x}] \bullet \delta\underline{\mathbf{Y}}[\mathbf{x}] - \mathbf{b}(\mathbf{x}) \cdot \delta\mathbf{y}(\mathbf{x})) \, dV_{\mathbf{x}} \\ &= \int_{\mathcal{B}} \left( \int_{\mathcal{B}} \hat{W}_{\underline{\mathbf{Y}}}[\mathbf{x}]\langle \mathbf{q} - \mathbf{x} \rangle \cdot (\delta\mathbf{y}(\mathbf{q}) - \delta\mathbf{y}(\mathbf{x})) \, dV_{\mathbf{q}} - \mathbf{b}(\mathbf{x}) \cdot \delta\mathbf{y}(\mathbf{x}) \right) \, dV_{\mathbf{x}}. \end{aligned}$$

Using the change of dummy variables $\mathbf{q} \leftrightarrow \mathbf{x}$ to eliminate $\delta\mathbf{y}(\mathbf{q})$,

$$0 = \int_{\mathcal{B}} \left( \int_{\mathcal{B}} (\hat{W}_{\underline{\mathbf{Y}}}[\mathbf{q}]\langle \mathbf{x} - \mathbf{q} \rangle - \hat{W}_{\underline{\mathbf{Y}}}[\mathbf{x}]\langle \mathbf{q} - \mathbf{x} \rangle) \, dV_{\mathbf{q}} - \mathbf{b}(\mathbf{x}) \right) \cdot \delta\mathbf{y}(\mathbf{x}) \, dV_{\mathbf{x}}.$$

Since this must hold for every choice of the variation $\delta\mathbf{y}$, the Euler-Lagrange equation, which is the peridynamic equilibrium equation, is given by

$$\mathbf{L}^{\mathrm{pd}}(\mathbf{x}) + \mathbf{b}(\mathbf{x}) = \mathbf{0} \tag{1-5}$$

for all $\mathbf{x} \in \mathcal{B}$. Here, the *peridynamic internal force density* at $\mathbf{x}$ is given by

$$\mathbf{L}^{\mathrm{pd}}(\mathbf{x}) = \int_{\mathcal{B}} \left\{ \underline{\mathbf{T}}[\mathbf{x}]\langle \mathbf{q}-\mathbf{x}\rangle - \underline{\mathbf{T}}[\mathbf{q}]\langle \mathbf{x}-\mathbf{q}\rangle \right\} dV_{\mathbf{q}} \tag{1-6}$$

where $\underline{\mathbf{T}}[\mathbf{x}]$ is the *force state* at $\mathbf{x}$, which is related to the strain energy density by

$$\underline{\mathbf{T}}[\mathbf{x}] = \hat{W}_{\underline{\mathbf{Y}}}(\underline{\mathbf{Y}}[\mathbf{x}]). \tag{1-7}$$

The *pairwise bond force density* $\mathbf{f}$ on a point $\mathbf{x}$ due to interaction with any point $\mathbf{q} \in \mathcal{F}_{\mathbf{x}}$ is given by

$$\mathbf{f}(\mathbf{q},\mathbf{x}) = \underline{\mathbf{T}}[\mathbf{x}]\langle \mathbf{q}-\mathbf{x}\rangle - \underline{\mathbf{T}}[\mathbf{q}]\langle \mathbf{x}-\mathbf{q}\rangle. \tag{1-8}$$

The internal force density (1-6) may be written more succinctly in terms of the pairwise bond force density:

$$\mathbf{L}^{\mathrm{pd}}(\mathbf{x}) = \int_{\mathcal{B}} \mathbf{f}(\mathbf{q},\mathbf{x})\, dV_{\mathbf{q}}. \tag{1-9}$$

In general,

$$\underline{\mathbf{T}}[\mathbf{x}] = \hat{\underline{\mathbf{T}}}(\underline{\mathbf{Y}}[\mathbf{x}]), \qquad \underline{\mathbf{T}}[\mathbf{q}] = \hat{\underline{\mathbf{T}}}(\underline{\mathbf{Y}}[\mathbf{q}])$$

where $\hat{\underline{\mathbf{T}}}$ is the material model expressed in terms of the force state.

By invoking d'Alembert's principle, the dynamic form of the balance of linear momentum is found from (1-5) to be

$$\rho(\mathbf{x})\ddot{\mathbf{y}}(\mathbf{x},t) = \mathbf{L}^{\mathrm{pd}}(\mathbf{x},t) + \mathbf{b}(\mathbf{x},t) \tag{1-10}$$

for all $\mathbf{x} \in \mathcal{B}$ and for any $t$, where $\rho$ is the mass density.

The mechanical interpretation of the force state is that $\underline{\mathbf{T}}[\mathbf{x}]\langle \mathbf{q}-\mathbf{x}\rangle$ represents a bond force density on $\mathbf{x}$ due to its interaction with $\mathbf{q}$. More general material models, whether elastic or not, may be written in the form

$$\underline{\mathbf{T}}[\mathbf{x}] = \hat{\underline{\mathbf{T}}}(\underline{\mathbf{Y}}[\mathbf{x}], \ldots, \mathbf{x})$$

where $\hat{\underline{\mathbf{T}}}$ is the material model, which may depend on additional variables besides $\underline{\mathbf{Y}}$. The dimensions of $\underline{\mathbf{T}}$ and $\mathbf{f}$ are $FL^{-6}$, or equivalently $MT^{-2}L^{-5}$. The dimensions of $W$ are the same as in the standard theory, $FL^{-2}$ or $MT^{-2}L^{-1}$.

If at any $\mathbf{x}$, $\underline{\mathbf{T}}$ depends only on $\underline{\mathbf{Y}}$ (but not additional variables such as loading history), then the material model is *simple*, and we write

$$\underline{\mathbf{T}}[\mathbf{x}] = \hat{\underline{\mathbf{T}}}(\underline{\mathbf{Y}}[\mathbf{x}], \mathbf{x}).$$

All elastic materials are simple.

If $\hat{\underline{\mathbf{T}}}$ has no explicit dependence on $\mathbf{x}$, then the body is *homogeneous*. If it is simple and homogeneous, we write

$$\underline{\mathbf{T}}[\mathbf{x}] = \hat{\underline{\mathbf{T}}}(\underline{\mathbf{Y}}[\mathbf{x}]).$$

Since $\delta$ is in effect a material property, any homogeneous body has constant $\delta$.

If $\delta$ is constant on $\mathcal{B}$, then the region of integration in (1-6) and (1-9) may be changed from $\mathcal{B}$ to $\mathcal{F}_{\mathbf{x}}$. The vast majority of applications of peridynamics to date assume constant horizon.

## 2. Peridynamic stress tensor

As shown in [8], the peridynamic internal force density can be expressed without approximation as

$$\mathbf{L}^{\mathrm{pd}} = \nabla \cdot \boldsymbol{\nu}^{\mathrm{pd}} \qquad \text{on } \mathcal{B}$$

where $\boldsymbol{\nu}^{\mathrm{pd}}$ is the *peridynamic stress tensor* field defined for any $\mathbf{x}$ by

$$\boldsymbol{\nu}^{\mathrm{pd}}(\mathbf{x}) = \frac{1}{2}\int_{\mathcal{S}}\int_0^\infty\int_0^\infty (v+w)^2 \mathbf{f}(\mathbf{x}+v\mathbf{m}, \mathbf{x}-w\mathbf{m}) \otimes \mathbf{m}\, dw\, dv\, d\Omega_{\mathbf{m}} \tag{2-1}$$

where $\mathcal{S}$ is the unit sphere, $d\Omega_{\mathbf{m}}$ is a differential solid angle in the direction of the unit vector $\mathbf{m}$, and $\mathbf{f}$ is given by (1-8).

Suppose the deformation is continuously differentiable, and let $\mathbf{F}$ be the usual deformation gradient tensor field,

$$\mathbf{F} = \nabla \mathbf{y} \qquad \text{on } \mathcal{B}.$$

Define the *deformation gradient state* field $\underline{\mathbf{F}}$ by

$$\underline{\mathbf{F}}[\mathbf{x}]\langle \boldsymbol{\xi}\rangle = \mathbf{F}(\mathbf{x})\boldsymbol{\xi} \qquad \forall \mathbf{x} \in \mathcal{B},\ \boldsymbol{\xi} \in \mathcal{H}_{\mathbf{x}}. \tag{2-2}$$

An equivalent statement is

$$\underline{\mathbf{F}} = \mathbf{F}\underline{\mathbf{X}} \qquad \text{on } \mathcal{B}$$

where $\underline{\mathbf{X}}$ is the *identity* state defined by

$$\underline{\mathbf{X}}\langle \boldsymbol{\xi}\rangle = \boldsymbol{\xi} \qquad \forall \boldsymbol{\xi} \in \mathcal{H}_{\mathbf{x}}.$$

Suppose the deformation is such that there is a tensor $\mathbf{F}^*$ such that

$$\mathbf{y}(\mathbf{x}+\boldsymbol{\xi}) - \mathbf{y}(\mathbf{x}) = \mathbf{F}^*\boldsymbol{\xi} \qquad \forall \mathbf{x} \in \mathcal{B},\ \boldsymbol{\xi} \in \mathcal{H}_{\mathbf{x}}.$$

Then the deformation is called *uniform*. In this case,

$$\underline{\mathbf{Y}} = \underline{\mathbf{F}} \quad \text{on } \mathcal{B}, \qquad \underline{\mathbf{F}}[\mathbf{x}]\langle \boldsymbol{\xi}\rangle = \mathbf{F}^*\boldsymbol{\xi} \qquad \forall \mathbf{x} \in \mathcal{B},\ \boldsymbol{\xi} \in \mathcal{H}_{\mathbf{x}}. \tag{2-3}$$

If the body is homogeneous and the deformation is uniform, then the peridynamic stress tensor is easily computed making use of the change of variables $z = v + w$:

$$\begin{aligned}
\boldsymbol{\nu}^{\mathrm{pd}} &= \int_{\mathcal{S}}\int_0^\infty\int_v^\infty z^2 \hat{\underline{\mathbf{T}}}(\underline{\mathbf{F}})\langle z\mathbf{m}\rangle \otimes \mathbf{m}\, dz\, dv\, d\Omega_{\mathbf{m}} \\
&= \int_{\mathcal{S}}\int_0^\infty\int_0^z z^2 \hat{\underline{\mathbf{T}}}(\underline{\mathbf{F}})\langle z\mathbf{m}\rangle \otimes \mathbf{m}\, dv\, dz\, d\Omega_{\mathbf{m}} \\
&= \int_{\mathcal{S}}\int_0^\infty z^3 \hat{\underline{\mathbf{T}}}(\underline{\mathbf{F}})\langle z\mathbf{m}\rangle \otimes \mathbf{m}\, dz\, d\Omega_{\mathbf{m}} \\
&= \int_{\mathcal{S}}\int_0^\infty \hat{\underline{\mathbf{T}}}(\underline{\mathbf{F}})\langle z\mathbf{m}\rangle \otimes (z\mathbf{m})(z^2\, dz\, d\Omega_{\mathbf{m}}) \\
&= \boldsymbol{\nu}^0
\end{aligned} \tag{2-4}$$

where $\boldsymbol{\nu}^0$ is the *collapsed stress tensor* defined by

$$\boldsymbol{\nu}^0 = \int_{\mathcal{H}} \hat{\underline{\mathbf{T}}}(\underline{\mathbf{F}})\langle \boldsymbol{\xi}\rangle \otimes \boldsymbol{\xi}\, dV_{\boldsymbol{\xi}}. \tag{2-5}$$

Also define the *collapsed internal force density* field by

$$\mathbf{L}^0 = \nabla \cdot \boldsymbol{\nu}^0 \qquad \text{on } \mathcal{B}. \tag{2-6}$$

As discussed in [27], the collapsed stress tensor is an admissible first Piola-Kirchhoff stress tensor whose constitutive model depends on the local deformation gradient tensor through (2-5). The

collapsed internal force density field provides the "local limit of peridynamics" in the sense that as $\delta \to 0$,

$$\mathbf{L}^{\mathrm{pd}} \to \mathbf{L}^0$$

provided the deformation is twice continuously differentiable and $\underline{\hat{\mathbf{T}}}$ obeys the scaling relation derived in the next section.

## 3. Rescaling a material model at a point

The remainder of this paper concerns methods for allowing changes in the horizon as a function of position such that the "bulk properties" are invariant to this change. The first step is to specify what this required invariance means.

Suppose an elastic material model is given for a particular value of horizon (without loss of generality, we will assume that this horizon is 1), and call the strain energy density function $\hat{W}_1$. Now consider a different value of horizon $\delta$, and call the modified strain energy density function $\hat{W}$. As a physical requirement, the strain energy density for any uniform deformation must be invariant with respect to changes in $\delta$. By reasoning similar to that in [27], it is assumed that for any deformation state $\underline{\mathbf{Y}}$,

$$\hat{W}(\underline{\mathbf{Y}}) = \hat{W}_1(\underline{\mathbf{Y}}_1) \tag{3-1}$$

where $\underline{\mathbf{Y}}_1$ is the *reference deformation state* defined by

$$\underline{\mathbf{Y}}_1\langle \mathbf{n} \rangle = \delta^{-1}\underline{\mathbf{Y}}\langle \delta\mathbf{n} \rangle \qquad \forall \mathbf{n} \in \mathcal{H}_1 \tag{3-2}$$

where $\mathcal{H}_1$ is the family of $\mathbf{x}$ with horizon 1. (In the remainder of this paper, the symbols $\mathbf{n}$ or $\mathbf{m}$ will generally be used instead of $\boldsymbol{\xi}$ to denote bonds in $\mathcal{H}_1$.) To derive the force state $\underline{\mathbf{T}}$, observe that (3-1) implies

$$\hat{W}_{\underline{\mathbf{Y}}} \bullet d\underline{\mathbf{Y}} = (\hat{W}_1)_{\underline{\mathbf{Y}}_1} \bullet d\underline{\mathbf{Y}}_1.$$

Hence, using (1-7),

$$\underline{\mathbf{T}} \bullet d\underline{\mathbf{Y}} = \underline{\mathbf{T}}_1 \bullet d\underline{\mathbf{Y}}_1.$$

Combining this with (1-2), (1-3), and (3-2) leads to the following scaling relation for peridynamic material models in three dimensions:

$$\underline{\hat{\mathbf{T}}}(\underline{\mathbf{Y}})\langle \boldsymbol{\xi} \rangle = \delta^{-4}\underline{\hat{\mathbf{T}}}_1(\underline{\mathbf{Y}}_1)\langle \delta^{-1}\boldsymbol{\xi} \rangle \qquad \forall \boldsymbol{\xi} \in \mathcal{H}$$

for any deformation state $\underline{\mathbf{Y}}$ on $\mathcal{H}$. Repeating the above derivation for 1- or 2-dimensional models leads to

$$\underline{\hat{\mathbf{T}}}(\underline{\mathbf{Y}})\langle \boldsymbol{\xi} \rangle = \delta^{-(1+D)}\underline{\hat{\mathbf{T}}}_1(\underline{\mathbf{Y}}_1)\langle \delta^{-1}\boldsymbol{\xi} \rangle \qquad \forall \boldsymbol{\xi} \in \mathcal{H} \tag{3-3}$$

where $D$ is the number of dimensions and $\underline{\mathbf{Y}}_1$ is given by (3-2). $\underline{\hat{\mathbf{T}}}_1$ is called the *reference material model*.

From (2-2) and (3-2), the deformation gradient state has the following invariance with respect to changes in $\delta$:

$$\underline{\mathbf{F}}_1\langle \mathbf{n} \rangle = \delta^{-1}\underline{\mathbf{F}}\langle \delta\mathbf{n} \rangle = \delta^{-1}\mathbf{F}\delta\mathbf{n} = \mathbf{F}\mathbf{n} = \underline{\mathbf{F}}\langle \mathbf{n} \rangle \qquad \forall \mathbf{n} \in \mathcal{H}_1$$

hence

$$\underline{\mathbf{F}}_1 = \underline{\mathbf{F}} \qquad \text{on } \mathcal{H} \cap \mathcal{H}_1, \tag{3-4}$$

which is a result that could be anticipated owing to the fact that $\mathbf{F}$ is dimensionless. From (2-5), (3-2) and (3-3),

$$\begin{aligned}\boldsymbol{\nu}^0 &= \int_{\mathcal{H}} \hat{\underline{\mathbf{T}}}(\underline{\mathbf{F}})\langle\boldsymbol{\xi}\rangle \otimes \boldsymbol{\xi}\, dV_{\boldsymbol{\xi}} \\ &= \int_{\mathcal{H}_1} \delta^{-(1+D)} \hat{\underline{\mathbf{T}}}_1(\underline{\mathbf{F}}_1)\langle\mathbf{n}\rangle \otimes (\delta\mathbf{n})(\delta^D dV_{\mathbf{n}}) \\ &= \int_{\mathcal{H}_1} \hat{\underline{\mathbf{T}}}_1(\underline{\mathbf{F}}_1)\langle\mathbf{n}\rangle \otimes \mathbf{n}\, dV_{\mathbf{n}} \end{aligned} \tag{3-5}$$

which shows that the collapsed stress tensor is also invariant with respect to changes in $\delta$. (This invariance does not require that the body be homogeneous.)

## 4. Variable scale homogeneous bodies

Recall from Section 1 that any homogeneous body necessarily has constant horizon. So, it is necessary to define a relaxed concept of homogeneity that captures what it means for a peridynamic body to have constant "bulk properties" without adhering to the strict definition of homogeneity. The reference material model defined in the previous section provides a way to do this.

*Definition.* Suppose a reference material model $\hat{\underline{\mathbf{T}}}_1$ is given in $\mathcal{B}$, independent of position. Also let the horizon $\delta(\mathbf{x})$ be prescribed as a function of position. If, at any $\mathbf{x} \in \mathcal{B}$,

$$\hat{\underline{\mathbf{T}}}(\underline{\mathbf{Y}}[\mathbf{x}], \mathbf{x})\langle\boldsymbol{\xi}\rangle = \frac{1}{(\delta(\mathbf{x}))^{1+D}} \hat{\underline{\mathbf{T}}}_1(\underline{\mathbf{Y}}_1[\mathbf{x}]) \left\langle \frac{\boldsymbol{\xi}}{\delta(\mathbf{x})} \right\rangle \qquad \boldsymbol{\xi} \in \mathcal{H}_{\mathbf{x}}, \tag{4-1}$$

then $\mathcal{B}$ is a *variable scale homogeneous* (VSH) body. (A homogeneous body is a VSH body with constant horizon.)

By the results of Section 3, an elastic VSH body under uniform deformation has constant $W$. However, it does *not* necessarily have constant $\boldsymbol{\nu}^{\mathrm{pd}}$ and is therefore not necessarily in equilibrium in the absence of body forces. (Recall that (2-4) applies only to homogeneous bodies, and homogeneity implies that $\delta$ is constant.) As shown in the next section, non-constant $\delta$ in a VSH body leads to *ghost forces* at points where the horizon changes.

## 5. Ghost forces

Here we demonstrate that in the absence of body forces, a uniform deformation of a VSH body is not necessarily in equilibrium. To see this, assume that $\delta$ is twice continuously differentiable, and compute the net internal force density $\mathbf{L}^{\mathrm{pd}}(\mathbf{x})$. From (1-6) and (4-1), for any $\mathbf{x}$,

$$\begin{aligned}\mathbf{L}^{\mathrm{pd}}(\mathbf{x}) &= \int \{\underline{\mathbf{T}}[\mathbf{x}]\langle\mathbf{q}-\mathbf{x}\rangle - \underline{\mathbf{T}}[\mathbf{q}]\langle\mathbf{x}-\mathbf{q}\rangle\}\, dV_{\mathbf{q}} \\ &= \int \left\{\delta^{-(1+D)}(\mathbf{x})\underline{\mathbf{T}}_1\langle\mathbf{m}\rangle - \delta^{-(1+D)}(\mathbf{q})\underline{\mathbf{T}}_1\langle\mathbf{n}\rangle\right\} dV_{\mathbf{q}} \end{aligned} \tag{5-1}$$

where

$$\mathbf{m} = \frac{\mathbf{q}-\mathbf{x}}{\delta(\mathbf{x})}, \qquad \mathbf{n} = \frac{\mathbf{x}-\mathbf{q}}{\delta(\mathbf{q})}. \tag{5-2}$$

(In this section, all volume integrals are over $\mathbb{R}^3$.) Holding $\mathbf{x}$ fixed,

$$dV_{\mathbf{q}} = \left|\det\left(\frac{\partial \mathbf{m}}{\partial \mathbf{q}}\right)\right|^{-1} dV_{\mathbf{m}} = \delta^D(\mathbf{x}) dV_{\mathbf{m}}, \tag{5-3}$$

$$dV_{\mathbf{q}} = \left|\det\left(\frac{\partial \mathbf{n}}{\partial \mathbf{q}}\right)\right|^{-1} dV_{\mathbf{n}} = \frac{\delta^D(\mathbf{q})}{1 + \mathbf{n}\cdot\nabla\delta(\mathbf{q}) + O(|\nabla\delta|^2)} dV_{\mathbf{n}}. \tag{5-4}$$

From (5-1), (5-2), (5-3), and (5-4), it follows that

$$\begin{aligned} \mathbf{L}^{\mathrm{pd}}(\mathbf{x}) &= \int \frac{\underline{\mathbf{T}}_1\langle \mathbf{m}\rangle}{\delta(\mathbf{x})}\, dV_{\mathbf{m}} - \int \frac{\underline{\mathbf{T}}_1\langle \mathbf{n}\rangle}{\delta(\mathbf{q})}\left(\frac{1}{1 + \mathbf{n}\cdot\nabla\delta(\mathbf{q}) + O(|\nabla\delta|^2)}\right) dV_{\mathbf{n}} \\ &= \int \epsilon(\mathbf{x},\mathbf{q})\underline{\mathbf{T}}_1\langle \mathbf{m}\rangle\, dV_{\mathbf{m}} \end{aligned} \tag{5-5}$$

where

$$\begin{aligned} \epsilon(\mathbf{x},\mathbf{q}) &= \frac{1}{\delta(\mathbf{x})} - \frac{1}{\delta(\mathbf{q})}\left(\frac{1}{1 + \mathbf{n}\cdot\nabla\delta(\mathbf{q}) + O(|\nabla\delta|^2)}\right) \\ &= \frac{1}{\delta(\mathbf{x})} - \frac{1}{\delta(\mathbf{q}) + \nabla\delta(\mathbf{q})\cdot(\mathbf{x}-\mathbf{q}) + O(\delta|\nabla\delta|^2)}. \end{aligned} \tag{5-6}$$

Now approximate $\delta(\mathbf{x})$ by the first three terms of a Taylor expansion centered at $\mathbf{q}$, that is,

$$\delta(\mathbf{x}) = \delta(\mathbf{q}) + \nabla\delta(\mathbf{q})\cdot(\mathbf{x}-\mathbf{q}) + \nabla\nabla\delta(\mathbf{q})(\boldsymbol{\xi}\otimes\boldsymbol{\xi})/2 + \dots$$

where $\boldsymbol{\xi} = \mathbf{q} - \mathbf{x}$. Using this to eliminate the term $\nabla\delta(\mathbf{q})\cdot(\mathbf{x}-\mathbf{q})$ in (5-6) leads, after further straightforward manipulations, to

$$\begin{aligned} \epsilon(\mathbf{x},\mathbf{q}) &= \frac{1}{\delta(\mathbf{x})} - \frac{1}{\delta(\mathbf{x}) - \nabla\nabla\delta(\mathbf{q})(\boldsymbol{\xi}\otimes\boldsymbol{\xi})/2 + \dots} \\ &= -\frac{1}{2}\nabla\nabla\delta(\mathbf{q})\mathbf{m}\otimes\mathbf{m} + \dots \end{aligned}$$

where $\mathbf{m}$ is again given by (5-2). From this result and (5-5), the internal force density at $\mathbf{x}$ is estimated from

$$\mathbf{L}^{\mathrm{pd}}(\mathbf{x}) = -\frac{1}{2}\int \nabla\nabla\delta(\mathbf{q})(\mathbf{m}\otimes\mathbf{m})\underline{\mathbf{T}}_1\langle \mathbf{m}\rangle\, dV_{\mathbf{m}} + \dots$$

hence,

$$|\mathbf{L}^{\mathrm{pd}}(\mathbf{x})| \le \frac{1}{2}\int \max_{\mathcal{H}_{\mathbf{x}}}\Big\{|\nabla\nabla\delta|\Big\}|\mathbf{m}\otimes\mathbf{m}||\underline{\mathbf{T}}_1\langle \mathbf{m}\rangle|\, dV_{\mathbf{m}} + \dots.$$

Since, by assumption, $\delta$ is twice continuously differentiable, and since $|\mathbf{m}| \le 1$, this result implies

$$\mathbf{L}^{\mathrm{pd}}(\mathbf{x}) = O(|\nabla\nabla\delta|)O(\|\underline{\mathbf{T}}_1\|). \tag{5-7}$$

The departure from equilibrium represented by nonzero values of $\mathbf{L}^{\mathrm{pd}}$ is called *ghost force* and is an artifact of the position dependence of the horizon. Observe that the leading term in the ghost force depends on the *second* derivative of $\delta$. In fact, it can be shown directly that if $\delta$ is a linear function of position, then the ghost force vanishes.

An illustration of the effect of ghost force in a VSH bar in equilibrium is shown in Figure 1. The peridynamic reference material model $\underline{\hat{\mathbf{T}}}_1$ is a bond-based model [22] with a nominal Young's modulus of 1. The horizon in the bar depends on position as shown in the top figure. The numerical approximation method is discussed in the Appendix. Two cases are considered for dependence of the horizon: piecewise linear ("not smoothed") and cubic spline ("smoothed"). The ends of the bar have prescribed displacements corresponding to a nominal strain in the bar

of 1. The strain (defined as $du/dx$) in equilibrium for the two cases is shown in the lower figure (strain is computed numerically using a central finite difference formula). If there were no ghost forces, the strain would be constant and equal to 1. Because of ghost forces, anomalies in strain ("ghost strains") appear that equilibrate the ghost forces. The smoothed $\delta(x)$ has lower ghost strains than the non-smoothed case. This result is consistent with (5-7), which predicts ghost forces proportional to the second derivative of $\delta(x)$.

In this example, the anomalies in strain are less than 2%, even for the non-smoothed case. This departure from constant strain could be acceptable in many applications. Ghost forces in a VSH peridynamic body are always self-equilibrated: they do not exert a net force on the body. This follows from the fact that the peridynamic equilibrium equation always conserves linear momentum, even if the material model depends on position. To address applications in which these ghost forces are not acceptable, or it is desired to have a jump in $\delta(x)$, we will introduce two methods, *partial stress* and *splice* that exhibit zero ghost forces in a uniform deformation of a VSH body.

## 6. Partial stress field

Here we investigate a modified form of the momentum balance that eliminates ghost forces in a VSH body under uniform deformation. The momentum balance is expressed in terms of a new field called the "partial stress" tensor field.

Consider a peridynamic body $\mathcal{B}$ and let its force state field $\underline{\mathbf{T}}$ be given. Let the *partial stress* tensor field $\boldsymbol{\nu}^{\mathrm{ps}}$ be defined by

$$\boldsymbol{\nu}^{\mathrm{ps}}(\mathbf{x}) = \int_{\mathcal{H}_{\mathbf{x}}} \underline{\mathbf{T}}[\mathbf{x}]\langle \boldsymbol{\xi} \rangle \otimes \boldsymbol{\xi} \, dV_{\boldsymbol{\xi}} \qquad \forall \mathbf{x} \in \mathcal{B}. \tag{6-1}$$

Also define the *partial internal force density* by

$$\mathbf{L}^{\mathrm{ps}}(\mathbf{x}) = \nabla \cdot \boldsymbol{\nu}^{\mathrm{ps}}(\mathbf{x}) \qquad \forall \mathbf{x} \in \mathcal{B}. \tag{6-2}$$

If the material model is simple, the partial stress can be expressed in the form

$$\boldsymbol{\nu}^{\mathrm{ps}}(\mathbf{x}) = \hat{\boldsymbol{\nu}}^{\mathrm{ps}}(\underline{\mathbf{Y}}[\mathbf{x}]) \qquad \forall \mathbf{x} \in \mathcal{B}$$

where

$$\hat{\boldsymbol{\nu}}^{\mathrm{ps}}(\underline{\mathbf{Y}}) = \int_{\mathcal{H}} \hat{\underline{\mathbf{T}}}(\underline{\mathbf{Y}})\langle \boldsymbol{\xi} \rangle \otimes \boldsymbol{\xi} \, dV_{\boldsymbol{\xi}}. \tag{6-3}$$

Note the similarity between $\boldsymbol{\nu}^{\mathrm{ps}}$ and $\boldsymbol{\nu}^0$ defined by (2-5). The difference is that $\boldsymbol{\nu}^{\mathrm{ps}}$ depends on the (nonlocal) deformation state $\underline{\mathbf{Y}}$, while $\boldsymbol{\nu}^0$ depends on the (local) deformation gradient tensor. In the special case of a uniform deformation of a homogeneous body (which implies $\delta =$ constant and $\underline{\mathbf{Y}} = \underline{\mathbf{F}}$), clearly $\boldsymbol{\nu}^{\mathrm{ps}} \equiv \boldsymbol{\nu}^0$.

By repeating the manipulations leading to (3-5), it is easily shown that in a VSH body with reference material model $\hat{\underline{\mathbf{T}}}_1$,

$$\boldsymbol{\nu}^{\mathrm{ps}}(\mathbf{x}) = \int_{\mathcal{H}_1} \hat{\underline{\mathbf{T}}}_1(\underline{\mathbf{Y}}_1[\mathbf{x}])\langle \mathbf{n} \rangle \otimes \mathbf{n} \, dV_{\mathbf{n}} \qquad \forall \mathbf{x} \in \mathcal{B} \tag{6-4}$$

where $\underline{\mathbf{Y}}_1$ is given by (3-2). Since, in a uniform deformation, $\underline{\mathbf{Y}}_1$ is constant (and equal to $\underline{\mathbf{F}}$), it follows from (2-3), (2-6), (3-4), (3-5), (6-2), and (6-4) that in a VSH body under uniform deformation,

$$\boldsymbol{\nu}^{\mathrm{ps}} \equiv \boldsymbol{\nu}^0 \equiv \mathbf{0}, \qquad \mathbf{L}^{\mathrm{ps}} \equiv \mathbf{L}^0 \equiv \mathbf{0}. \tag{6-5}$$

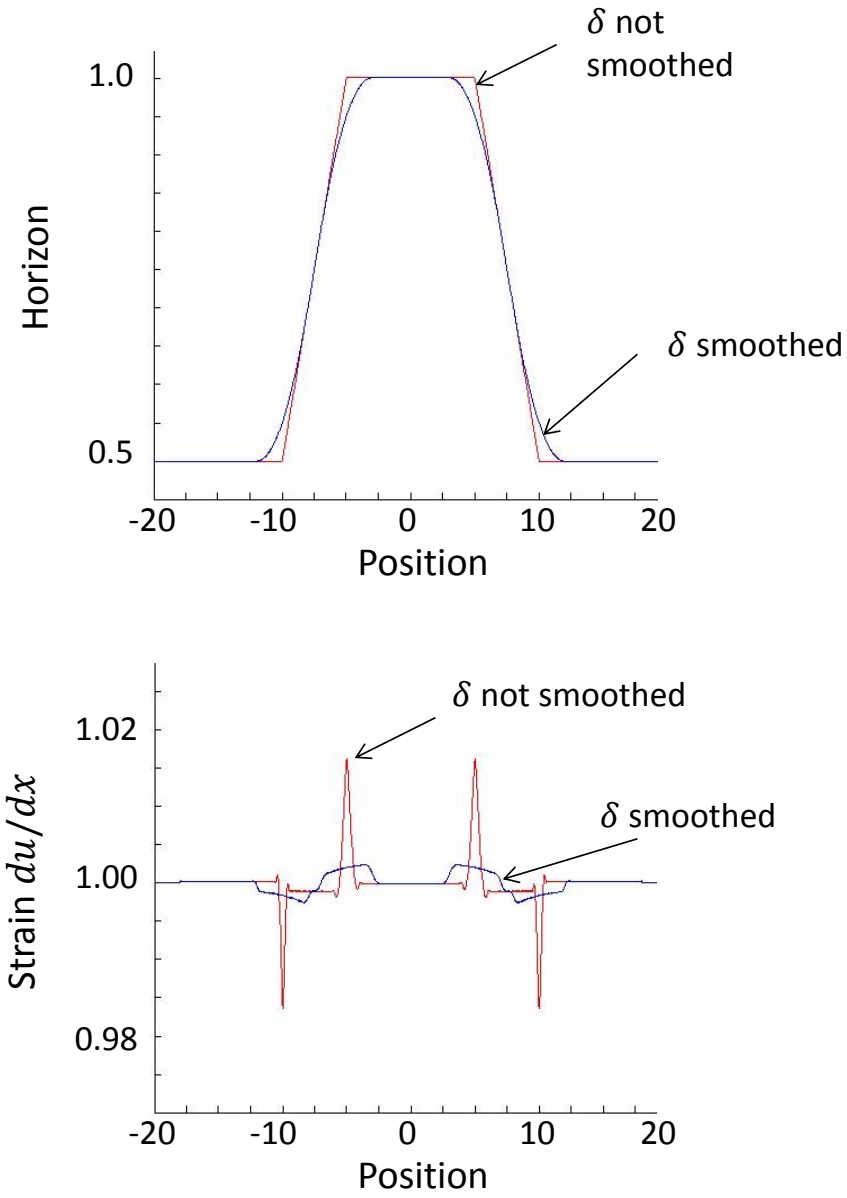


FIGURE 1. Ghost strain in a VSH body in equilibrium. Top: horizon as a function of position. Bottom: strain as a function of position.

This establishes that, for a VSH body under uniform deformation, ghost forces are absent in the partial stress formulation of the momentum balance equation. This observation motivates the use of this modified momentum balance in the transition region of the horizon.

## 7. Partial stress as an approximation to peridynamics

With the intent of modeling some parts of a body using partial internal force density (6-2) and other parts using the peridynamic internal force density (1-6), the relation between the two will now be investigated. Since the plan is to make a transition between $\mathbf{L}^{\text{ps}}$ and $\mathbf{L}^{\text{pd}}$ where the horizon is constant, we investigate the way these fields approximate each other under this assumption.

*Proposition 1.* Let $\mathcal{B}$ be a homogeneous body (which implies constant $\delta$). Let a twice continuously differentiable deformation $\mathbf{y}$ of $\mathcal{B}$ be prescribed. Then

*(i)*

$$\boldsymbol{\nu}^{\text{pd}} - \boldsymbol{\nu}^{\text{ps}} = O(\delta)O(\|\nabla \underline{\mathbf{T}}_1\|) \quad \text{on } \mathcal{B}, \tag{7-1}$$

*(ii)*

$$\mathbf{L}^{\text{pd}} - \mathbf{L}^{\text{ps}} = O(\delta)O(\|\nabla\nabla \underline{\mathbf{T}}_1\|) \quad \text{on } \mathcal{B}. \tag{7-2}$$

*Proof of (i).* Let $\mathbf{x} \in \mathcal{B}$ be fixed. Combining (1-8), (2-1), and (4-1), and setting $v = \delta v_1$, $w = \delta w_1$ leads to

$$\begin{aligned}
\boldsymbol{\nu}^{\text{pd}}(\mathbf{x}) &= \int_{\mathcal{S}} \int_0^\infty \int_0^\infty (v+w)^2 \underline{\mathbf{T}}[\mathbf{x} - w\mathbf{m}]\langle (v+w)\mathbf{m}\rangle \otimes \mathbf{m} \, dw \, dv \, d\Omega_{\mathbf{m}} \\
&= \int_{\mathcal{S}} \int_0^\infty \int_0^\infty (v_1+w_1)^2 \underline{\mathbf{T}}_1[\mathbf{x} - \delta w_1\mathbf{m}]\langle (v_1+w_1)\mathbf{m}\rangle \otimes \mathbf{m} \, dw_1 \, dv_1 \, d\Omega_{\mathbf{m}}.
\end{aligned}$$

The first two terms of a Taylor expansion for $\underline{\mathbf{T}}_1$ yield

$$\underline{\mathbf{T}}_1[\mathbf{x} - \delta w_1 \mathbf{m}] = \underline{\mathbf{T}}_1[\mathbf{x}] - \delta w_1 \nabla \underline{\mathbf{T}}_1[\mathbf{x}]\mathbf{m} + \dots.$$

After repeating the manipulations leading up to (2-4), the first term in this Taylor expansion, and after evaluating the triple integral, gives the partial stress defined by (6-1). Thus

$$\boldsymbol{\nu}^{\text{pd}} = \boldsymbol{\nu}^{\text{ps}} + O(\delta)O(\|\nabla \underline{\mathbf{T}}_1\|),$$

proving (7-1).

*Proof of (ii).* Let $\mathbf{x} \in \mathcal{B}$ be fixed. Applying a Taylor expansion to $\underline{\mathbf{T}}$ near $\mathbf{x}$ and setting $\boldsymbol{\xi} = \mathbf{q} - \mathbf{x}$ leads to

$$\underline{\mathbf{T}}[\mathbf{q}] = \underline{\mathbf{T}}[\mathbf{x}] + \nabla \underline{\mathbf{T}}[\mathbf{x}]\boldsymbol{\xi} + \frac{1}{2}\nabla\nabla \underline{\mathbf{T}}[\mathbf{x}](\boldsymbol{\xi} \otimes \boldsymbol{\xi}) + \dots.$$

Combining this with (1-6),

$$\begin{aligned}
\mathbf{L}^{\text{pd}}(\mathbf{x}) &= \int_{\mathcal{H}} \Big\{ \underline{\mathbf{T}}[\mathbf{x}]\langle \boldsymbol{\xi}\rangle - \underline{\mathbf{T}}[\mathbf{q}]\langle -\boldsymbol{\xi}\rangle \Big\} \, dV_{\boldsymbol{\xi}} \\
&= \int_{\mathcal{H}} \Big\{ \underline{\mathbf{T}}[\mathbf{x}]\langle \boldsymbol{\xi}\rangle - \big( \underline{\mathbf{T}}[\mathbf{x}]\langle -\boldsymbol{\xi}\rangle + \nabla \underline{\mathbf{T}}[\mathbf{x}]\langle -\boldsymbol{\xi}\rangle \boldsymbol{\xi} \\
&\qquad + \frac{1}{2}\nabla\nabla \underline{\mathbf{T}}[\mathbf{x}]\langle -\boldsymbol{\xi}\rangle(\boldsymbol{\xi} \otimes \boldsymbol{\xi}) + \dots \big) \Big\} \, dV_{\boldsymbol{\xi}}.
\end{aligned}$$

Replacing $\boldsymbol{\xi}$ by $-\boldsymbol{\xi}$, the first two terms in the integrand cancel. Bringing the gradient operator in the third term of the integrand outside of the integral yields

$$\begin{aligned}\mathbf{L}^{\mathrm{pd}}(\mathbf{x}) &= \nabla\cdot\int_{\mathcal{H}_{\mathbf{x}}}\underline{\mathbf{T}}[\boldsymbol{\xi}]\langle\boldsymbol{\xi}\rangle\otimes\boldsymbol{\xi}\,dV_{\boldsymbol{\xi}}-\frac{1}{2}\int_{\mathcal{H}_{\mathbf{x}}}\nabla\nabla\underline{\mathbf{T}}[\mathbf{x}]\langle\boldsymbol{\xi}\rangle\cdot(\boldsymbol{\xi}\otimes\boldsymbol{\xi})\,dV_{\boldsymbol{\xi}}+\dots\\ &= \mathbf{L}^{\mathrm{ps}}(\mathbf{x})-\frac{1}{2}\int_{\mathcal{H}_{\mathbf{x}}}\nabla\nabla\underline{\mathbf{T}}[\mathbf{x}]\langle\boldsymbol{\xi}\rangle\cdot(\boldsymbol{\xi}\otimes\boldsymbol{\xi})\,dV_{\boldsymbol{\xi}}+\dots\end{aligned}$$

Using (3-3) to express the remainder in terms of the reference force state, and setting $\boldsymbol{\xi}=\delta\mathbf{m}$, this implies

$$\mathbf{L}^{\mathrm{pd}}(\mathbf{x})=\mathbf{L}^{\mathrm{ps}}(\mathbf{x})-\frac{\delta}{2}\int_{\mathcal{H}_1}\nabla\nabla\underline{\mathbf{T}}_1[\mathbf{x}]\langle\mathbf{m}\rangle\cdot(\mathbf{m}\otimes\mathbf{m})\,dV_{\mathbf{m}}+\dots$$

Since $|\mathbf{m}|\le 1$, this proves (7-2). □

Because of (7-2), it follows that at the interface between subregions where $\mathbf{L}^{\mathrm{ps}}$ and $\mathbf{L}^{\mathrm{pd}}$ are used in the momentum balance, there are no ghost forces if the deformation is uniform (since $\underline{\mathbf{T}}_1$ is constant on $\mathcal{B}$).

Figure 2 shows an example in which the horizon is a function of position in a VSH bar. The horizon increases from 0.1 on the left to 1.0 on the right through a transition region of thickness 0.1. The numerical approximation method is discussed in the Appendix. An incident wave pulse is applied on the left boundary. The total thickness of the pulse is 4.0, which is thin enough that we expect to see some effect of nonlocality as the pulse moves into the high-$\delta$ region. Two cases are considered: (1) the full peridynamic equations applied throughout the domain, and (2) the partial stress model is applied in a region containing and surrounding the transition region. In case (2), the total width of the partial stress region is 10, and the full peridynamic equations are applied everywhere else. Figure 3 compares the time history of the displacement at the point $x=-10$ for the two cases, showing both the incident and reflected pulse. Evidently, the use of partial stress in the transition region reduces the reflections. Figure 4 shows the comparison at the point $x=10$, showing the transmitted pulses, which are essentially the same for both models. The change in shape of the transmitted pulse compared with the incident pulse is primarily due to nonlocality: as $\delta$ increases, short wavelength components of the pulse experience a lower wave speed. This effect of nonlocality on wave speed is reflected in dependence on horizon of dispersion curves for linear waves [26, 21].

This example illustrates that it is hopeless to try to find a coupling method that transmits waves without reflection between regions with different horizons. However, as the example demonstrates, different coupling methods can have different transmission and reflection properties that may be more or less desirable for different applications.

## 8. Partial stress as an approximation to the local theory

In Section 7, the relationship between the partial stress and the full peridynamic versions of the internal force density were discussed. Here, we investigate the approximate relationship between the partial stress formulation and the local theory. The appropriate material model in the local theory uses the collapsed stress tensor defined by (2-5), because, as shown in (6-5), it coincides with the partial stress for uniform deformations.

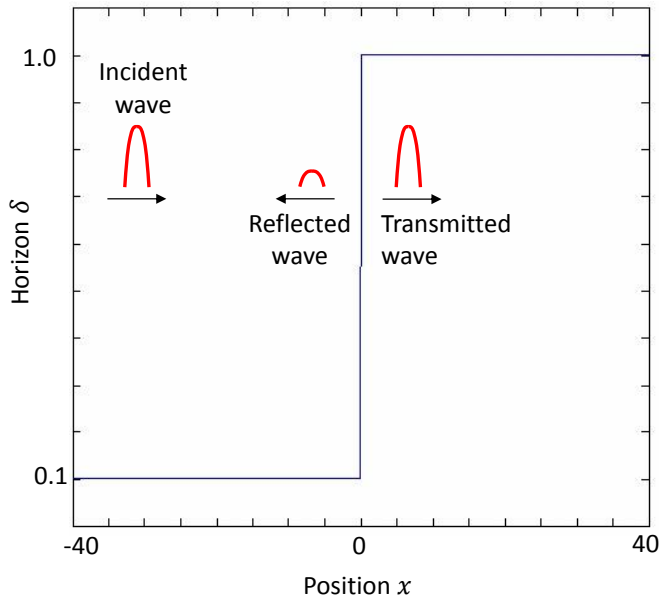


FIGURE 2. Stress pulse in a VSH bar: horizon as a function of position.

*Proposition 2.* Let $\mathcal{B}$ be a homogeneous body (which implies constant $\delta$). Let the reference material model $\underline{\hat{\mathbf{T}}}_1$ be a continuously differentiable function (of the reference deformation state). Let $\mathbf{y}$ be twice continuously differentiable on $\mathcal{B}$. Then

*(i)*

$$\boldsymbol{\nu}^{\mathrm{ps}} - \boldsymbol{\nu}^0 = O(\delta)O(\|\nabla \underline{\mathbf{T}}_1\|) \qquad \text{on } \mathcal{B} \tag{8-1}$$

where $\boldsymbol{\nu}^{\mathrm{ps}}$ and $\boldsymbol{\nu}^0$ are defined by (6-1) and (2-5), and

*(ii)*

$$\mathbf{L}^{\mathrm{ps}} - \mathbf{L}^0 = O(\delta)O(\|\nabla\nabla \underline{\mathbf{T}}_1\|) \qquad \text{on } \mathcal{B} \tag{8-2}$$

where $\mathbf{L}^{\mathrm{ps}}$ and $\mathbf{L}^0$ are defined by (6-2) and (2-6).

*Proof of (i).* Let $\mathbf{x} \in \mathcal{B}$ be fixed. From (3-2) and a Taylor expansion of $\mathbf{y}$ near $\mathbf{x}$,

$$\begin{aligned} \underline{\mathbf{Y}}_1[\mathbf{x}]\langle \mathbf{n} \rangle &= \delta^{-1}(\mathbf{y}(\mathbf{x} + \delta\mathbf{n}) - \mathbf{y}(\mathbf{x})) \\ &= \delta^{-1}\Big((\mathbf{y}(\mathbf{x}) + \delta\mathbf{F}(\mathbf{x})\mathbf{n} + \delta^2\nabla\mathbf{F}(\mathbf{x})(\mathbf{n}\otimes\mathbf{n})/2 + \dots) - \mathbf{y}(\mathbf{x})\Big). \\ &= \mathbf{F}(\mathbf{x})\mathbf{n} + \delta\nabla\mathbf{F}(\mathbf{x})(\mathbf{n}\otimes\mathbf{n})/2 + \dots \end{aligned}$$

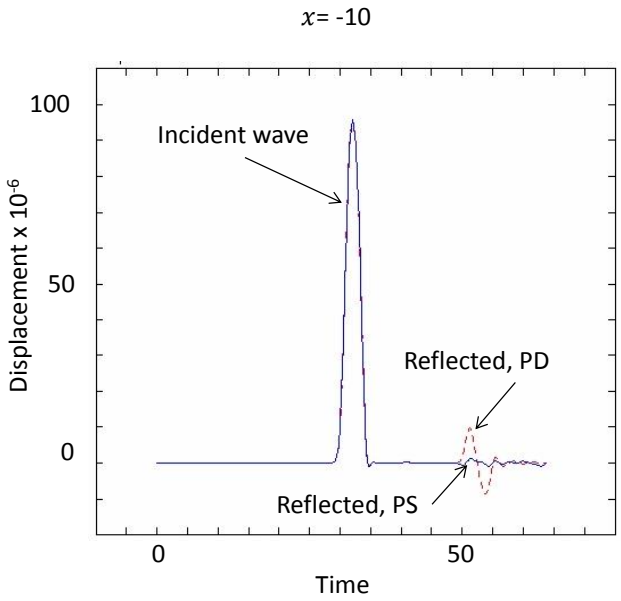


FIGURE 3. Stress pulse in a VSH bar: time history of displacement at $x = -10$. The two curves are for a fully peridynamic (PD) model, and for peridynamic with a partial stress (PS) region surrounding the transition in $\delta$. The PS curve has a different reflection than the PD model.

hence

$$\underline{\mathbf{Y}}_1 = \underline{\mathbf{F}} + O(\delta)O(\|\nabla\underline{\mathbf{F}}\|) \tag{8-3}$$

and similarly

$$\nabla\underline{\mathbf{Y}}_1 = \nabla\underline{\mathbf{F}} + O(\delta)O(\|\nabla\nabla\underline{\mathbf{F}}\|). \tag{8-4}$$

By the chain rule for Fréchet derivatives and (8-4),

$$\begin{aligned} \nabla\underline{\mathbf{T}}_1 &= \underline{\mathbb{K}} \bullet \nabla\underline{\mathbf{Y}}_1 \\ &= \underline{\mathbb{K}} \bullet (\nabla\underline{\mathbf{F}} + O(\delta)O(\|\nabla\nabla\underline{\mathbf{F}}\|)) \end{aligned} \tag{8-5}$$

where $\underline{\mathbb{K}} = (\hat{\underline{\mathbf{T}}}_1)_{\underline{\mathbf{Y}}_1}$, that is, the Fréchet derivative of $\hat{\underline{\mathbf{T}}}_1$ (also known as the *micromodulus double state* [23]). From (8-5), it is immediate that

$$O(\|\nabla\underline{\mathbf{T}}_1\|) = O(\|\nabla\underline{\mathbf{F}}\|). \tag{8-6}$$

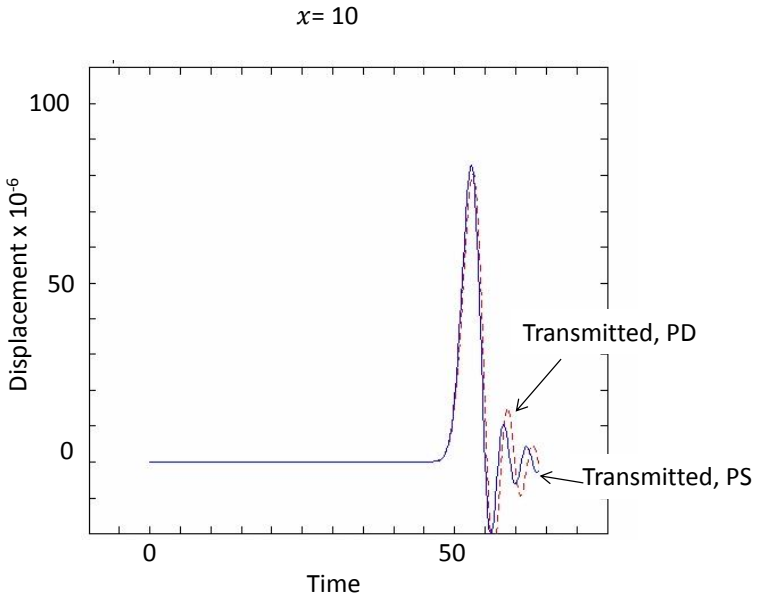


FIGURE 4. Stress pulse in a VSH bar: time history of displacement at $x = 10$. The transmitted pulses are similar between the two models, with the primary effect being the nonlocality of the material model.

From (8-3), (8-6), and a Taylor expansion of $\hat{\underline{\mathbf{T}}}_1$ near $\underline{\mathbf{Y}}_1$, it follows that

$$\begin{aligned}\hat{\underline{\mathbf{T}}}_1(\underline{\mathbf{Y}}_1) &= \hat{\underline{\mathbf{T}}}_1(\underline{\mathbf{F}}) + \mathbb{K} \bullet (\underline{\mathbf{Y}}_1 - \underline{\mathbf{F}}) + \dots \\ &= \hat{\underline{\mathbf{T}}}_1(\underline{\mathbf{F}}) + O(\delta)O(\|\nabla \underline{\mathbf{F}}\|) \\ &= \hat{\underline{\mathbf{T}}}_1(\underline{\mathbf{F}}) + O(\delta)O(\|\nabla \underline{\mathbf{T}}_1\|). \end{aligned} \tag{8-7}$$

From (2-5), (6-4), and (8-7),

$$\begin{aligned}\boldsymbol{\nu}^{\mathrm{ps}}(\mathbf{x}) &= \int_{\mathcal{H}_1} \hat{\underline{\mathbf{T}}}_1(\underline{\mathbf{Y}}[\mathbf{x}])\langle \mathbf{n} \rangle \otimes \mathbf{n}\, dV_{\mathbf{n}} \\ &= \int_{\mathcal{H}_1} \left( \hat{\underline{\mathbf{T}}}_1(\underline{\mathbf{F}}[\mathbf{x}])\langle \mathbf{n} \rangle + O(\delta)O(\|\nabla \underline{\mathbf{T}}_1\|) \right) \otimes \mathbf{n}\, dV_{\mathbf{n}} \\ &= \int_{\mathcal{H}_1} \hat{\underline{\mathbf{T}}}_1(\underline{\mathbf{F}}[\mathbf{x}])\langle \mathbf{n} \rangle \otimes \mathbf{n}\, dV_{\mathbf{n}} + O(\delta)O(\|\nabla \underline{\mathbf{T}}_1\|) \\ &= \boldsymbol{\nu}^0(\mathbf{x}) + O(\delta)O(\|\nabla \underline{\mathbf{T}}_1\|) \end{aligned}$$

which proves (8-1).

The proof of *(ii)* is similar to the above, making use of the relations $\mathbf{L}^{\mathrm{ps}} = \nabla \cdot \boldsymbol{\nu}^{\mathrm{ps}}$ and $\mathbf{L}^0 = \nabla \cdot \boldsymbol{\nu}^0$. $\square$

Since $\hat{\underline{\mathbf{T}}}_1$ is constant in a VSH body under uniform deformation, (8-1) and (8-2) imply (6-5), provided the conditions of Proposition 2 are satisfied.

Comparing (7-1) with (8-1), and comparing (7-2) with (8-2), it follows that under the conditions of Proposition 2 (which are stronger than those of Proposition 1),

$$\boldsymbol{\nu}^{\mathrm{pd}} - \boldsymbol{\nu}^0 = O(\delta)O(\|\nabla \underline{\mathbf{T}}_1\|) \quad \text{on } \mathcal{B}, \tag{8-8}$$

$$\mathbf{L}^{\mathrm{pd}} - \mathbf{L}^0 = O(\delta)O(\|\nabla\nabla \underline{\mathbf{T}}_1\|) \quad \text{on } \mathcal{B}. \tag{8-9}$$

This result is consistent with the conclusion in [27] that the collapsed internal force density is the "local limit of peridynamics."

## 9. Splice between two peridynamic subregions

Let two values of horizon be denoted $\delta_+$ and $\delta_-$, and assume $\delta_- \le \delta_+$. Let a reference material model $\hat{\underline{\mathbf{T}}}_1$ be given. Suppose, for a given deformation, two force state fields are computed everywhere using (3-3). For any $\mathbf{x} \in \mathcal{B}$,

$$\underline{\mathbf{T}}_+[\mathbf{x}]\langle\boldsymbol{\xi}\rangle = \frac{1}{\delta_+^{1+D}}\hat{\underline{\mathbf{T}}}_1(\underline{\mathbf{Y}}_1[\mathbf{x}])\langle\boldsymbol{\xi}/\delta_+\rangle, \qquad \underline{\mathbf{T}}_-[\mathbf{x}]\langle\boldsymbol{\xi}\rangle = \frac{1}{\delta_-^{1+D}}\hat{\underline{\mathbf{T}}}_1(\underline{\mathbf{Y}}_1[\mathbf{x}])\langle\boldsymbol{\xi}/\delta_-\rangle.$$

Further suppose that $\mathcal{B}$ is divided into two disjoint subregions $\mathcal{B}_+$ and $\mathcal{B}_-$ and that the internal force density at any $\mathbf{x} \in \mathcal{B}$ is given by

$$\mathbf{L}(\mathbf{x}) = \mathbf{L}^{\mathrm{splice}}(\mathbf{x}) := \begin{cases} \int_{\mathcal{B}} \left\{\underline{\mathbf{T}}_+[\mathbf{x}]\langle\mathbf{q}-\mathbf{x}\rangle - \underline{\mathbf{T}}_+[\mathbf{q}]\langle\mathbf{x}-\mathbf{q}\rangle\right\} dV_{\mathbf{q}} & \text{if } \mathbf{x} \in \mathcal{B}_+, \\ \int_{\mathcal{B}} \left\{\underline{\mathbf{T}}_-[\mathbf{x}]\langle\mathbf{q}-\mathbf{x}\rangle - \underline{\mathbf{T}}_-[\mathbf{q}]\langle\mathbf{x}-\mathbf{q}\rangle\right\} dV_{\mathbf{q}} & \text{if } \mathbf{x} \in \mathcal{B}_-. \end{cases}$$

The resulting model of $\mathcal{B}$ is called a *splice* of the subregions $\mathcal{B}_+$ and $\mathcal{B}_-$.

A splice is not the same as a VSH with $\delta(\mathbf{x})$ prescribed as a step function. The difference is that in a splice, a point $\mathbf{x}$ near the interface "sees" the force states on the other side of the interface corresponding to the same value of horizon as itself, $\delta(\mathbf{x})$. In contrast, in a VSH, each point is assigned a unique value of horizon, and the force state at each point is uniquely computed according to this horizon.

In many applications, a splice provides a viable and convenient way to model a VSH body that has piecewise constant values of horizon. It is immediate that a splice model has zero internal force density under homogeneous deformation, since the values of $\underline{\mathbf{T}}_+$ and $\underline{\mathbf{T}}_-$ are constant throughout $\mathcal{B}_+$ and $\mathcal{B}_-$ respectively. This implies that a splice model produces no ghost forces under uniform deformation. This is the main advantange of a splice over a VSH body. The splice is similar to an adaptivity concept for 1D bond-based peridynamics proposed by Bobaru et al. [4] and in 2D by Bobaru and Ha [3]. A related approach has been used in the context of atomistic-to-continuum coupling by Seleson and Gunzburger [18].

It follows from Proposition 2 that in a splice, recalling that $\delta_- \le \delta_+$,

$$\boldsymbol{\nu}^{\mathrm{pd}}{}_+ - \boldsymbol{\nu}^{\mathrm{pd}}{}_- = O(\delta_+)O(\|\nabla \underline{\mathbf{T}}_1\|) \qquad \text{on } \mathcal{B}$$

and

$$\mathbf{L}^{\mathrm{pd}}{}_+ - \mathbf{L}^{\mathrm{pd}}{}_- = O(\delta_+)O(\|\nabla\nabla \underline{\mathbf{T}}_1\|) \quad \text{on } \mathcal{B}$$

provided that the conditions of Proposition 2 are satisfied.

## 10. Local-nonlocal coupling

The situation frequently arises that we wish to model most of a body using the standard local theory, and only a small portion (such as in the vicinity of a growing crack) with peridynamics. A method for achieving the transition between the two is called *local-nonlocal coupling*. Methods that have been proposed for local-nonlocal coupling include Arlequin [7], morphing [12, 1, 2], and blending [17, 20]. Liu and Hong proposed a coupling method using interface elements [11]. Methods that achieve coupling by treating peridynamic bonds as finite elements are described in Macek and Silling [13] and the book chapter by Oterkus and Madenci [14] which contains additional references. Related issues for nonlocal diffusion are investigated by Seleson, Gunzburger, and Parks [19]. Wu investigates a local-nonlocal coupling method for correspondence materials in state-based peridynamics [29]. An adaptive method for coupling peridynamic and local regions is discussed by Wildman and Gazonas [28].

One option for local-nonlocal coupling is to use the partial stress field as a bridge between local and peridynamic subregions. In this approach, $\mathcal{B}$ is divided into disjoint subregions $\mathcal{B}_0$, $\mathcal{B}_{\rm ps}$, and $\mathcal{B}_{\rm pd}$. To avoid ghost forces under uniform deformation, $\delta > 0$ is assumed to be constant in $\mathcal{B}_{\rm pd}$. Changes in $\delta$ occur entirely within $\mathcal{B}_{\rm ps}$, so that $\delta$ is continuous on $\mathcal{B}$. (Recall from (6-5) that $\boldsymbol{\nu}^{\rm ps} \equiv \boldsymbol{\nu}^0$ and $\mathbf{L}^{\rm ps} \equiv \mathbf{L}^0$ where $\delta \equiv 0$.) The internal force density is given by

$$\mathbf{L}(\mathbf{x}) = \begin{cases} \mathbf{L}^{\rm pd}(\mathbf{x}) & \text{if } \mathbf{x} \in \mathcal{B}_{\rm pd}, \\ \mathbf{L}^{\rm ps}(\mathbf{x}) & \text{if } \mathbf{x} \in \mathcal{B}_{\rm ps}, \\ \mathbf{L}^0(\mathbf{x}) & \text{if } \mathbf{x} \in \mathcal{B}_0. \end{cases} \tag{10-1}$$

The convergence properties of this method were derived in (7-2) and (8-2).

Another option for local-nonlocal coupling is to use the idea of a splice described in the previous section. The body is divided into disjoint subregions $\mathcal{B}_0$ and $\mathcal{B}_{\rm pd}$ that use the local model and the full peridynamic model (constant $\delta > 0$), respectively. The internal force density in the splice model is given by

$$\mathbf{L}(\mathbf{x}) = \begin{cases} \mathbf{L}^{\rm pd}(\mathbf{x}) & \text{if } \mathbf{x} \in \mathcal{B}_{\rm pd}, \\ \mathbf{L}^0(\mathbf{x}) & \text{if } \mathbf{x} \in \mathcal{B}_0. \end{cases} \tag{10-2}$$

The convergence properties of such a splice model are given by (8-9).

These two options for local-nonlocal coupling differ primarily in the way they transmit waves whose wavelength is smaller than or on the order of $\delta$. As illustrated in the example in Section 7, the transition from local to nonlocal always involves a change in the dispersion properties of the material, resulting in reflections of waves. However, because the partial stress coupling method (10-1) allows a gradual change in length scale, it can be used to reduce the reflections compared with the splice approach (10-2). As discussed in the Appendix, numerical computation of $\mathbf{L}^{\rm ps}$ requires the suppression of zero energy mode oscillations, similar to correspondence material models [9, 10, 5]. The root cause of these oscillations is the non-invertibility of $\hat{\boldsymbol{\nu}}^{\rm ps}(\underline{\mathbf{Y}})$, that is, there are many possible deformations of the family that result in the same partial stress tensor.

As an example, we apply these two methods for local-nonlocal coupling to the problem of spall initiated by the impact of two brittle elastic plates. The impactor has half the thickness of the target and strikes the target from the left side. As shown in the wave diagram in Figure 6, the compressive waves that issue from the contact surface between the impactor and the target eventually intersect each other at the midplane of the target plate. When this happens, the waves, which by that time are both tensile, reinforce each other to create a thin region where the stress is strongly tensile. Within this tensile region, the strength of the material is exceeded and a crack forms. The formation of this crack creates release pulses that move in both directions.

The velocity induced by the rightward-moving release pulse as it reflects from free surface of the target bar can be measured using VISAR or other techniques [6]. With the help of analysis or computational modeling, the exact characteristics of the crack release (or "pullback") pulse can be interpreted using suitable data processing techniques to reveal the dynamic stength properties of materials under strong tension (spall).

In the computational model of this spall experiment, the impactor and target plates have thicknesses of 20 and 40 respectively. The numerical solution method is described in the Appendix. The impact velocity is 0.1. The elastic modulus and density of both plates are 1. The reference material model $\underline{\hat{\mathbf{T}}}_1$ is the bond-based prototype microelastic brittle (PMB) material model [24] with a critical bond strain for failure of 0.04. The entire region is discretized into 1000 nodes. The objective is to model the relatively small part of the body where damage can occur using the full peridynamic equations. This peridynamic region is coupled to local regions using either of two methods:

- Partial stress: a peridynamic region of thickness 10, centered at the midpoint of the target plate, is enclosed by layers of thickness 4 where the partial stress method is applied. Beyond this, the local equations are used. In the peridynamic and partial stress regions, the horizon is $\delta = 0.13$.
- Splice: a peridynamic region of thickness 10 and horizon $\delta = 0.13$, centered at the midpoint of the target plate, is spliced to local regions.

For comparison, results using the full peridynamic model in the entire domain ($\delta = 0.13$ throughout) are also computed.

The computed velocity profile using the splice method for local-nonlocal coupling is shown in Figure 5. The time of this snapshot is $t = 70$. Comparing this figure with the wave diagram in Figure 6, a number of salient features may be seen. The crack appears as a sharp jump in velocity as a function of position $x = 40$. The two release (pullback) pulses move away from the crack at the wave velocity, which is $c = 1.0$. The computed velocity history at the free surface is shown in Figure 7. The dips in velocity represent the crack release pulse created in the interior of the target due to spall.

As shown in the figures, the three methods give nearly the same results in this example. However, a fully peridynamic model in multiple dimensions would require a much higher computational cost due to the large number of nonlocal interactions required to discretize the material model. So, in multiple dimensions, in problems where damage is confined to a small subregion, the splice or partial stress methods potentially offer a significant reduction in cost, while avoiding ghost forces. This anticipated cost reduction is a primary motivation for development of local-nonlocal coupling methods.

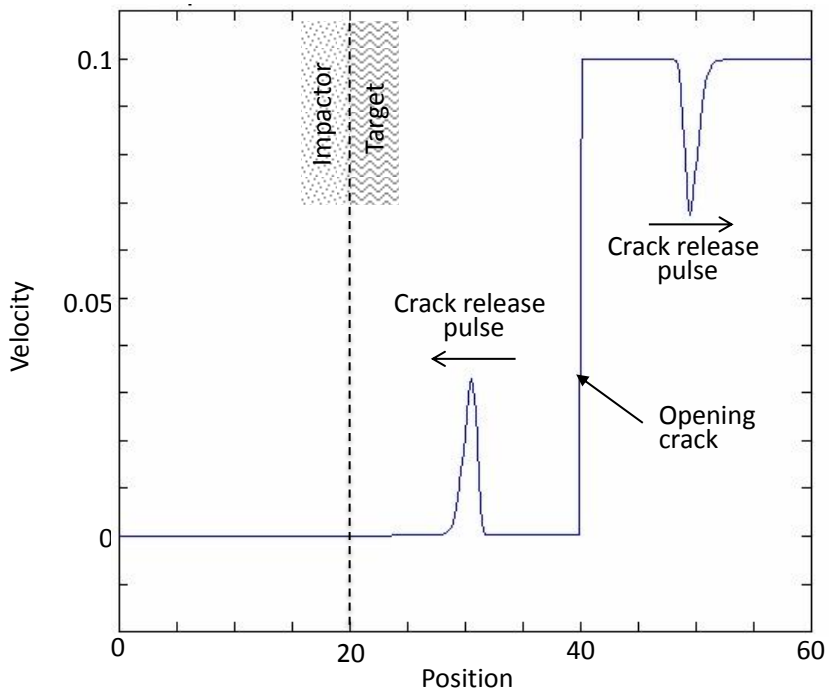


FIGURE 5. Velocity as a function of position at $t = 70$ in the spall example problem using the splice method for local-nonlocal coupling. There are no significant artifacts from the local-nonlocal transitions, which are located at $x = 37$ and $x = 43$.

## 11. Discussion

In this paper, we proposed a notion of a homogeneous body (a "variable scale homogeneous" body) that characterizes a peridynamic medium with variable horizon but with constant bulk material properties. We analyzed the origin and effect of ghost forces due to changes in the horizon in the full peridynamic model. The importance of these ghost forces depends on the application; they may or may not be acceptable in a computational simulation. These anomalies can be reduced by making $\delta(\mathbf{x})$ a smoothly varying function.

If the ghost forces under uniform deformation are not acceptable, the partial stress field can be used to effect a transition between regions with different horizon. The partial stress field appears

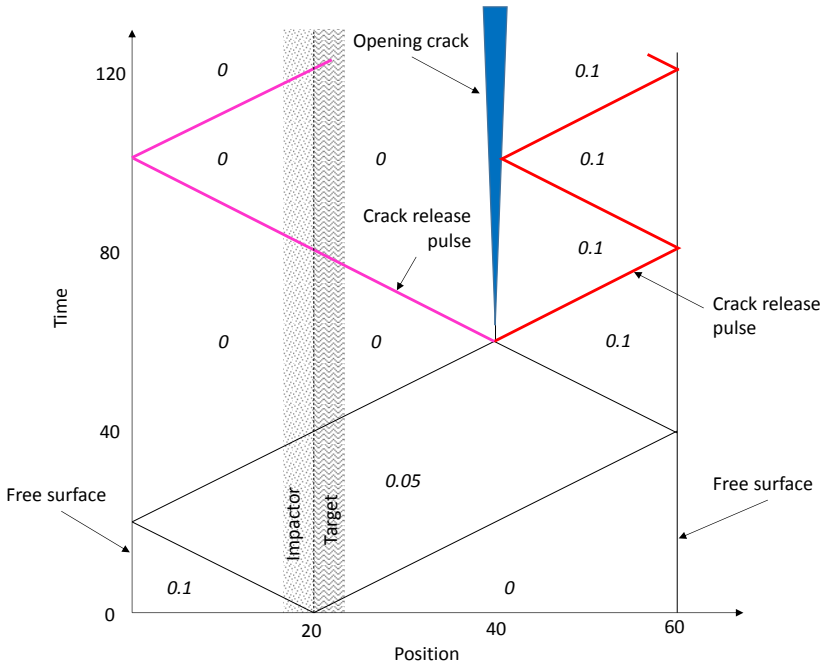


FIGURE 6. Wave diagram for the impact of a plate (from the left) on a target plate. Waves reinforce at the midplane of the target plate to cause fracture. Numbers in italics represent particle velocity.

in a modified form of the equilibrium equation. The partial stress approaches the collapsed stress in the limit of zero horizon, if the deformation is continuously differentiable. The collapsed stress $\hat{\boldsymbol{\nu}}^0(\mathbf{F})$ provides a material model for the first Piola-Kirchhoff stress in the local formulation.

The partial stress formulation is not thermodynamically consistent in the sense that along a cyclic loading path of a family in an elastic material, nonzero net work may appear:

$$\oint \hat{\boldsymbol{\nu}}^{\mathrm{ps}}(\underline{\mathbf{Y}}) \cdot d\mathbf{F} \neq 0. \tag{11-1}$$

(An exception is a uniform deformation, in which case $\underline{\mathbf{Y}} = \underline{\mathbf{F}}$.) The root cause of this inconsistency, which is evident in (11-1), is that the partial stress concept mixes local and nonlocal kinematics. The partial stress is therefore not suitable as a basis for a general theory of continuum mechanics. The full peridynamic theory, like the local theory, *is* thermodynamically consistent [26, 15, 16], that is,

$$\oint \underline{\hat{\mathbf{T}}}(\underline{\mathbf{Y}}) \bullet d\underline{\mathbf{Y}} = 0, \qquad \text{and} \qquad \oint \hat{\boldsymbol{\nu}}^0(\mathbf{F}) \cdot d\mathbf{F} = 0.$$

To connect subregions with constant $\delta$ to each other, or to achieve local-nonlocal coupling, subregions can be connected using a splice. This method allows the peridynamic material model in each subregion to "see" force states in the other subregion with the same horizon as itself. The methods proposed in this paper may provide a means to reduce the cost of modeling a crack with peridynamics by connecting it to a larger surrounding region that is modeled with the local theory.

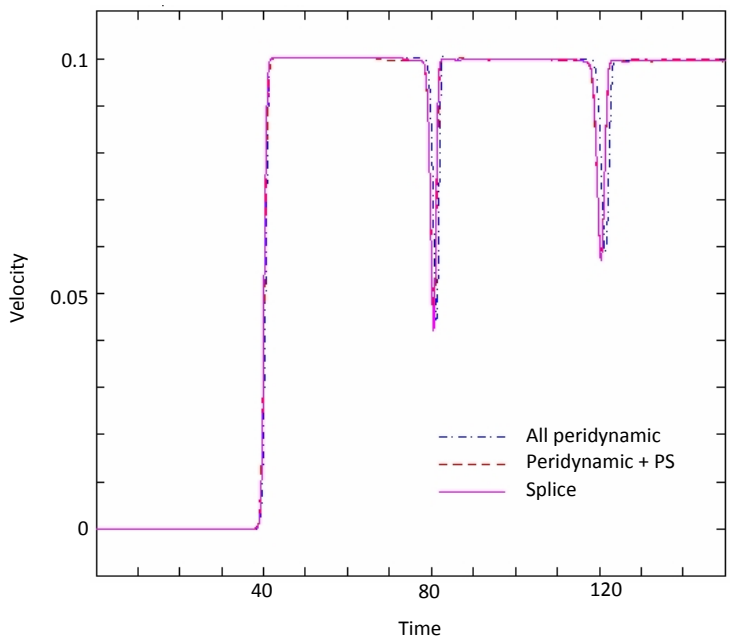


FIGURE 7. Velocity history at the free (right) surface of the target plate, showing the release pulse from the dynamic fracture occurring in the interior of the target bar. The three curves are for fully peridynamic (PD), local-nonlocal coupling using partial stress (PS), and local-nonlocal coupling using a splice.

## APPENDIX: COMPUTATIONAL DETAILS

All the numerical examples in this paper involving nonlocal models used the method described in [24]. This method uses a midpoint quadrature rule in a Lagrangian discretization of the body. The approximation in one dimension for the peridynamic internal force density is

$$L_i^{\mathrm{pd}} = \sum_{j \in \mathcal{F}_i} (T_{ij} - T_{ji}) V_j$$

where $i$ and $j$ are node numbers, $V_j$ is the volume of node $j$, $\mathcal{F}_i$ is the set of nodes in the material family of $i$, and

$$T_{ij} = \hat{\underline{T}}(\underline{Y}[x_i], x_i)\langle x_j - x_i \rangle, \qquad T_{ji} = \hat{\underline{T}}(\underline{Y}[x_j], x_j)\langle x_i - x_j \rangle,$$

$$\underline{Y}[x_i]\langle x_j - x_i \rangle = y_j - y_i, \qquad \underline{Y}[x_j]\langle x_i - x_j \rangle = y_i - y_j.$$

The partial stress is computed from

$$\nu_i^{\mathrm{ps}} = \sum_{j \in \mathcal{F}_i} T_{ij}(x_j - x_i)V_j.$$

The internal force density in the partial stress formulation is computed approximated by

$$L_i^{\mathrm{ps}} = \frac{\nu_{i+1}^{\mathrm{ps}} - \nu_{i-1}^{\mathrm{ps}}}{2\Delta x}$$

where $\Delta x$ is the mesh spacing. For computations involving the PDEs of the local theory, the Piola (collapsed) stress is approximated by the finite difference formula

$$\nu_{i+1/2}^0 = \hat{\nu}^0(F_{i+1/2}), \qquad F_{i+1/2} = \frac{y_{i+1} - y_i}{\Delta x}$$

where $\hat{\nu}^0$ is the material model for the Piola stress. The internal force density in the local model is approximated by

$$L_i^0 = \frac{\nu_{i+1/2}^0 - \nu_{i-1/2}^0}{\Delta x}.$$

For dynamics, time integration is performed using explicit central differencing:

$$v_i^{n+1/2} - v_i^{n-1/2} = a_i^n \Delta t,$$
$$y_i^{n+1} - y_i^n = v_i^{n+1/2} \Delta t$$

where $\Delta t$ is the time step size. At time step $n$, the acceleration is computed from

$$\rho a_i^n = L_i^n + b_i^n + \eta_i^n,$$

where $L$ is either $L^{\mathrm{pd}}$, $L^{\mathrm{ps}}$, or $L^0$, $\rho$ is density, $b$ is body force density, and $\eta$ is the linear artificial viscosity:

$$\eta_i^n = \alpha \rho c \Delta x (v_{i+1}^n - 2v_i^n + v_{i-1}^n)$$

where $c$ is the wave speed and $\alpha$ is a dimensionless constant on the order of $1/4$. The linear artificial viscosity is effective in reducing zero energy mode oscillations that can appear due to the non-invertibility of the partial stress tensor and, when a correspondence material model is used, of the peridynamic force state. Other methods for controlling zero energy mode oscillations are described by Breitenfeld *et al.* [5] and by Littlewood [9, 10]. Artificial viscosity $\eta_i^n$ is not applied if the bonds from $i$ to $i+1$ or $i$ to $i-1$ are damaged according to the material damage model at time step $n$. Otherwise, the artificial viscosity would create nonphysical forces across a crack surface.

## References


[1] Yan Azdoud, Fei Han, and Gilles Lubineau. A morphing framework to couple non-local and local anisotropic continua. *International Journal of Solids and Structures*, 50:1332–1341, 2013.

[2] Yan Azdoud, Fei Han, and Gilles Lubineau. The morphing method as a flexible tool for adaptive local/non-local simulation of static fracture. *Computational Mechanics*, pages 1–12, 2014.

[3] Florin Bobaru and Youn Doh Ha. Adaptive refinement and multiscale modeling in 2d peridynamics. *International Journal for Multiscale Computational Engineering*, 9(6), 2011.

[4] Florin Bobaru, Mijia Yang, Leonardo Frota Alves, Stewart A Silling, Ebrahim Askari, and Jifeng Xu. Convergence, adaptive refinement, and scaling in 1d peridynamics. *International Journal for Numerical Methods in Engineering*, 77(6):852–877, 2009.

[5] MS Breitenfeld, PH Geubelle, O Weckner, and SA Silling. Non-ordinary state-based peridynamic analysis of stationary crack problems. *Computer Methods in Applied Mechanics and Engineering*, 272:233–250, 2014.

[6] JE Field, SM Walley, WG Proud, HT Goldrein, and CR Siviour. Review of experimental techniques for high rate deformation and shock studies. *International Journal of Impact Engineering*, 30:725–775, 2004.

[7] Fei Han and Gilles Lubineau. Coupling of nonlocal and local continuum models by the Arlequin approach. *International Journal for Numerical Methods in Engineering*, 89:671–685, 2012.

[8] R. B. Lehoucq and S. A. Silling. Force flux and the peridynamic stress tensor. *Journal of the Mechanics and Physics of Solids*, 56:1566–1577, 2008.

[9] David J Littlewood. Simulation of dynamic fracture using peridynamics, finite element modeling, and contact. In *ASME 2010 International Mechanical Engineering Congress and Exposition*, pages 209–217. American Society of Mechanical Engineers, 2010.

[10] David J Littlewood. A nonlocal approach to modeling crack nucleation in aa 7075-t651. In *ASME 2011 International Mechanical Engineering Congress and Exposition*, pages 567–576. American Society of Mechanical Engineers, 2011.

[11] Wenyang Liu and Jung-Wuk Hong. A coupling approach of discretized peridynamics with finite element method. *Computer Methods in Applied Mechanics and Engineering*, 245:163–175, 2012.

[12] Gilles Lubineau, Yan Azdoud, Fei Han, Christian Rey, and Abe Askari. A morphing strategy to couple non-local to local continuum mechanics. *Journal of the Mechanics and Physics of Solids*, 60:1088–1102, 2012.

[13] R. W. Macek and S. A. Silling. Peridynamics via finite element analysis. *Finite Elements in Analysis and Design*, 43:1169–1178, 2007.

[14] Erdogan Madenci and Erkan Oterkus. Coupling of the peridynamic theory and finite element method. In *Peridynamic Theory and Its Applications*, pages 191–202. Springer, 2014.

[15] Selda Oterkus, Erdogan Madenci, and Abigail Agwai. Fully coupled peridynamic thermomechanics. *Journal of the Mechanics and Physics of Solids*, 64:1–23, 2014.

[16] Selda Oterkus, Erdogan Madenci, and Abigail Agwai. Peridynamic thermal diffusion. *Journal of Computational Physics*, 265:71–96, 2014.

[17] Pablo Seleson, Samir Beneddine, and Serge Prudhomme. A force-based coupling scheme for peridynamics and classical elasticity. *Computational Materials Science*, 66:34–49, 2013.

[18] Pablo Seleson and Max Gunzburger. Bridging methods for atomistic-to-continuum coupling and their implementation. *Communications in Computational Physics*, 7(4):831, 2010.

[19] Pablo Seleson, Max Gunzburger, and Michael L Parks. Interface problems in nonlocal diffusion and sharp transitions between local and nonlocal domains. *Computer Methods in Applied Mechanics and Engineering*, 266:185–204, 2013.

[20] Pablo Seleson, Youn Doh Ha, and Samir Beneddine. Concurrent coupling of bond-based peridynamics and the Navier equation of classical elasticity by blending. *International Journal for Multiscale Computational Engineering*, (to appear).

[21] Pablo Seleson and Michael Parks. On the role of the influence function in the peridynamic theory. *International Journal of Multiscale Computational Engineering*, 9(6):689–706, 2011.

[22] S. A. Silling. Reformulation of elasticity theory for discontinuities and long-range forces. *Journal of the Mechanics and Physics of Solids*, 48:175–209, 2000.

[23] S. A. Silling. Linearized theory of peridynamic states. *Journal of Elasticity*, 99:85–111, 2010.

[24] S. A. Silling and E. Askari. A meshfree method based on the peridynamic model of solid mechanics. *Computers and Structures*, 83:1526–1535, 2005.

[25] S. A. Silling, M. Epton, O. Weckner, J. Xu, and E. Askari. Peridynamic states and constitutive modeling. *Journal of Elasticity*, 88:151–184, 2007.

[26] S. A. Silling and R. B. Lehoucq. The peridynamic theory of solid mechanics. *Advances in Applied Mechanics*, 44:73–166, 2010.

[27] Stewart A. Silling and Richard B. Lehoucq. Convergence of peridynamics to classical elasticity theory. *Journal of Elasticity*, 93:13–37, 2008.

[28] Raymond A Wildman and George A Gazonas. A finite difference-augmented peridynamics method for reducing wave dispersion. *International Journal of Fracture*, 190(1-2):39–52, 2014.

[29] CT Wu. Kinematic constraints in the state-based peridynamics with mixed local/nonlocal gradient approximations. *Computational Mechanics*, 54(5):1255–1267, 2014.

Multiscale Science Department, Sandia National Laboratories, P.O. Box 5800, MS-1322, Albuquerque, NM 87185-1322, USA
*E-mail address*: sasilli@sandia.gov

Multiscale Science Department, Sandia National Laboratories, P.O. Box 5800, MS-1322, Albuquerque, NM 87185-1322, USA
*E-mail address*: djlittl@sandia.gov

Computer Science and Mathematics Division, Oak Ridge National Laboratory, P.O. Box 2008, Oak Ridge, TN 37831, USA
*E-mail address*: selesonpd@ornl.gov